ESTIMATING LEVER-TYPE ACTIVE MULTIPLE TUNED MASS DAMPERS FOR STRUCTURES UNDER HARMONIC EXCITATION

Chunxiang Li and Bingkang Han

ESTIMATING LEVER-TYPE ACTIVE MULTIPLE TUNED MASS DAMPERS FOR STRUCTURES UNDER HARMONIC EXCITATION

CHUNXIANG LI AND BINGKANG HAN

Lever-type active multiple tuned mass dampers (LT-AMTMD) consisting of several lever-type active tuned mass damper (LT-ATMD) units with a uniform distribution of natural frequencies have been proposed here for the vibration control of long-span bridges under the excitation directly acting on the structure, rather than through the base. The main purpose of selecting this form of excitation is to present guidelines for the buffeting control design of long-span bridges under wind loads. Estimations have been made on the performance of the LT-AMTMD with identical stiffness and damping coefficient and unequal masses for the reduction of harmonically forced vibrations by resorting to the defined evaluation criteria. The LT-AMTMD with the actuator set at the mass block is found to have better effectiveness and higher robustness in alleviating the vibrations of structures in comparison with the LT-AMTMD with the actuator set at any other location. A new major result is that both the spring static and dynamic stretching of the LT-AMTMD with the actuator set at the mass block may be freely adjusted in accordance with the practical requirements by changing the support locations within the viable range while practically maintaining the same performance. Numerical results demonstrate that the LT-AMTMD with the actuator set at the mass block can highly improve the performance of the LT-MTMD (that is, the passive counterpart of the LT-AMTMD) and provide better effectiveness than a single LT-ATMD. Estimations have also been simultaneously carried out on the LT-AMTMD (a single LT-ATMD) with respect to the hanging-type AMTMD (a single hanging-type ATMD) as well as on the LT-MTMD (a single LT-TMD) with reference to the hanging-type MTMD (a single hanging-type TMD), so as to highlight the improved performance of the proposed control system.

1. Introduction

The tuned mass damper (TMD) has been theoretically and experimentally corroborated to be effective in reducing the buffeting response of long-span bridges subjected to wind loads [Gu and Xiang 1992; Gu et al. 1994; Lin et al. 2000]. However, both large static and dynamic stretching of the spring in the hanging-type tuned mass damper (hanging-type TMD) may cause the spring to operate nonlinearly and the hanging-type TMD may not be fitted into the space available for installation within the bridge deck, consequently downgrading the performance and limiting the practical implementation of the hanging-type TMD. To overcome these shortcomings, the lever-type tuned mass damper (LT-TMD) has been proposed to deal with large static stretch of the spring in the hanging-type TMD [Gu et al. 1999]. In terms of the numerical results to be provided later on, the LT-TMD and the hanging-type TMD can approximately achieve the same effectiveness and mass block stroke. With respect to the hanging-type TMD, the LT-TMD, designed in accordance with the hypothesis-1 to be introduced later on, needs smaller

optimum damping ratio but significantly higher optimum tuning frequency ratio. However, the optimum parameters, effectiveness, and mass block stroke of the LT-TMD designed according to the hypothesis-2 to be introduced later on are approximately equal to those of the hanging-type TMD. As such, the LT-TMD can also not surmount the main disadvantage of the TMD (hanging-type TMD); that is, the sensitivity problem due to the fluctuation in tuning the natural frequency of the TMD (hanging-type TMD) to the controlled natural frequency of structures and (or) the offset in the optimum damping ratio of the hanging-type TMD. Furthermore, it has been demonstrated that both the dynamic responses and dynamic parameters of long-span bridges in terms of field measurements and wind tunnel tests and theoretical analyses are usually different from each other due in large part to the fact that the phenomenon of the wind-induced vibrations of long-span bridges is very complex [Diana et al. 1992; Conti et al. 1996].

In view of the above mentioned reasons, a more robust control device, such as the multiple tuned mass dampers (MTMD), which is able to control structural vibrations with variable natural frequencies, is needed for attaining a satisfying reduction of the buffeting response of long-span bridges under wind loads. As is well known, the MTMD with distributed natural frequencies were proposed by [Xu and Igusa 1992] and also investigated by many investigators such as [Yamaguchi and Harnpornchai 1993; Abe and Fujino 1994; Igusa and Xu 1994; Kareem and Kline 1995; Jangid 1995; Li 2000; Park and Reed 2001; Gu et al. 2001; Chen and Wu 2003; Kwon and Park 2004; Yau and Yang 2004; Hoang and Warnitchai 2005; Wang and Lin 2005; Lee et al. 2006]. The MTMD is confirmed to be capable of rendering better effectiveness and higher robustness in the mitigation of the oscillations of structures in comparison with a single TMD. Nevertheless, we note that if the hanging-type multiple tuned mass dampers (hanging-type MTMD) are directly used to suppress the buffeting response of long-span bridges, then each hanging-type TMD will possess both large static and dynamic stretching of the spring. Quantitatively, the static stretching of the spring of the jth hanging-type TMD in the hanging-type MTMD, h_j, can be determined in terms of the equation

$$h_j = g/(\omega_{Tj}^2),$$

where ω_{Tj} is the circular frequency of each hanging-type TMD and g refers to the acceleration due to gravity. Likewise, the maximum static stretching of the spring in the hanging-type MTMD is larger than the static stretching of a single hanging-type TMD with equal total mass ratio. Each LT-TMD in the lever-type multiple tuned mass dampers (LT-MTMD), proposed by the first author [Li and Li 2005], has the static stretching of the spring

$$h_j^* = \alpha[g/(\omega_{Tj}^2)] = \alpha h_j,$$

when the rigid arm is in a horizontal state. The numerical results to be stated later on demomstrate that the LT-MTMD designed in terms of the hypothesis-2 and the hanging-type MTMD have the approximately same effectiveness, robustness, and mass block stroke; but when the hanging-type MTMD is extended in terms of the hypothesis-1 to the LT-MTMD, the optimum tuning frequency ratio will change significantly while the optimum average damping ratio will show minor variations. A new basic result is that both the static and dynamic stretching of the spring in the LT-MTMD may be freely adjusted in accordance with the practical requirements through changing the support locations while approximately maintaining the same effectiveness, robustness, and mass block stroke.

Recently, a single lever-type active tuned mass damper (LT-ATMD) for mitigating harmonically forced vibrations has been recommended by [Li 2004] to acquire a control system with high effectiveness, in

which both the static and dynamic stretching of the spring may be freely adjusted to meet the practical requirements. The numerical results to be given next demonstrate that the LT-ATMD with the actuator set at the mass block can practically reach the same optimum damping ratio, optimum tuning frequency ratio, effectiveness, and mass block stroke as a single hanging-type ATMD. The LT-ATMD with the actuator set at the mass block is found to have much better effectiveness than the LT-TMD. More importantly, both the static and dynamic stretching of the spring in the LT-ATMD with the actuator set at the mass block may be freely adjusted in accordance with the practical requirements through changing the support locations, while approximately maintaining the same control performance (including the same mass block stroke). Further, the multiple active lever-type tuned mass dampers (MALTTMD), consisting of several active lever-type tuned mass damper (ALTTMD) units with a uniform distribution of natural frequencies, have been developed with the objective of attenuating the vibration control of long-span bridges under the ground acceleration, namely the external excitation acting on structures through the base [Li and Zhou 2004]. Taking into account that the probability of great drift of the controlled natural frequency may occur due to the complexity of the wind-induced vibrations of long-span bridges, a beforehand well-designed optimum LT-MTMD may result in the unsatisfactory effectiveness. This drawback can be surmounted by using the lever-type active multiple tuned mass dampers (LT-AMTMD). Therefore, there is a need for making an estimation of the LT-AMTMD with the aim of the external excitation directly acting on the structure, rather than through the base. Such a form of excitation is suitable for the buffeting control design of long-span bridges under wind loads, thereby giving guidelines for the buffeting control design of long-span bridges under wind loads.

The objective of this paper then is to evaluate the performance of the LT-AMTMD, including assessing the mass block stroke of the LT-AMTMD, in order to verify that the LT-AMTMD may also be a good candidate for the reduction of the buffeting response of long-span bridges with the consequence of not requiring both large static and dynamic stretching of the spring with respect to the hanging-type active multiple tuned mass dampers (hanging-type AMTMD) and possessing a desirable robustness in comparison with a single LT-ATMD. Estimations will also be simultaneously made on the LT-AMTMD / a single LT-ATMD with the actuator set at the mass block with respect to the hanging-type AMTMD / a single hanging-type ATMD, as well as on the LT-MTMD / a single LT-TMD with reference to the hanging-type MTMD / a single hanging-type TMD, so as to highlight both the improved performance and conspicuous feature of the proposed control system.

Nomenclature

ALTTMD	active lever-type tuned mass damper
c_s	mode-generalized damping coefficient of structures
c_T	constant damping coefficient of the LT-AMTMD
c_{Tj}	damping coefficient of the jth LT-ATMD in the LT-AMTMD
c_{tj}	velocity feedback gain of the jth LT-ATMD in the LT-AMTMD
DMF	dynamic magnification factors of the structure with the LT-AMTMD
DMF_j	dynamic magnification factors of the jth LT-ATMD in the LT-AMTMD
$F_{cj}(t)$	resultant force to act between the structure and jth LT-ATMD in the LT-AMTMD
F_s	frequency spacing of the LT-AMTMD, used for measuring its robustness

$F_{sj}(t)$	interaction force between the structure and support point of the jth LT-ATMD in the LT-AMTMD
f	tuning frequency ratio of the LT-AMTMD
$f(t)$	external excitation directly acting on the structure, rather than through the base
Hanging-type AMTMD	hanging-type active multiple tuned mass dampers
Hanging-type ATMD	Hanging-type active tuned mass damper
Hanging-type MTMD	hanging-type multiple tuned mass dampers
Hanging-type TMD	hanging-type tuned mass damper
$H_{y_s}(-i\omega)$	transfer function of the structure with the LT-AMTMD
$H_{y_{Tj}}(-i\omega)$	transfer function of the jth LT-ATMD in the LT-AMTMD
h_j	static stretching of the spring in the jth hanging-type TMD in the hanging-type MTMD
h_j^*	static stretching of the spring in the jth LT-TMD in the LT-AMTMD
$\mathrm{Im}(\omega)[\overline{\mathrm{Im}}(\omega)]$	imaginary part of a complex function, such as the transfer function of the structure with the LT-AMTMD
I_{Tj}	mass moment of inertia of the jth lever in the jth LT-ATMD
k_s	mode-generalized stiffness of structures
k_T	constant spring stiffness of the LT-AMTMD
k_{Tj}	spring stiffness of the jth LT-ATMD in the LT-AMTMD
k_{tj}	displacement feedback gain of the jth LT-ATMD in the LT-AMTMD
LT-AMTMD	lever-type active multiple tuned mass dampers
LT-ATMD	lever-type active tuned mass damper
LT-MTMD	lever-type multiple tuned mass dampers
LT-TMD	lever-type tuned mass damper
L_{T1j}	distance between the mass block and support point of the jth LT-ATMD
L_{T2j}	distance between the spring and support point of the jth LT-ATMD
L_{T3j}	distance between the active control force and mass block of the jth LT-ATMD
MALTTMD	multiple active lever-type tuned mass dampers
min . min . max . DMF	minimization of the minimum values of the maximum dynamic magnification factors of the structure with the LT-AMTMD
MTMD	multiple tuned mass dampers
m_j	lever mass of the jth LT-ATMD in the LT-AMTMD
m_s	mode-generalized mass of structures
m_{Tj}	mass of the jth LT-ATMD mass block
m_{tj}	acceleration feedback gain of the jth LT-ATMD in the LT-AMTMD
n	number of the LT-ATMD units in the LT-AMTMD
R_I	minimization of the minimum values of the maximum dynamic magnification factors (DMF) of the structure with the LT-AMTMD
$\mathrm{Re}(\omega)[\overline{\mathrm{Re}}(\omega)]$	real part of a complex function, such as the transfer function of the jth LT-ATMD in the LT-AMTMD

R_{m1}	ratio of the inertial force due to lever mass to that of block mass
R_{m2}	ratio of the moment of inertial force due to lever mass to that of block mass around the horizontal axis through the support point of the lever
R_{IIj}	maximum dynamic magnification factors (DMF) of the jth LT-ATMD (that is, mass block stroke)
R_{IIj}^*	spring stroke of the jth LT-ATMD in the LT-AMTMD
r_{Tj}	ratio of the natural frequency of the jth LT-ATMD to the structural natural frequency
r_{tj}	normalized acceleration feedback gain factor, NAFGF
r	constant normalized acceleration feedback gain factor, NAFGF
SDOF	single degree of freedom
TMD	tuned mass damper
y_{Tsj}	dynamic stretching of the spring in the jth LT-ATMD
y_s	displacement of the structure with respect to the ground
y_{Tj}	displacement of the jth LT-ATMD with reference to the structure
α	constant ratio of the distance between the spring and support point to that between the mass block and support point
α_j	ratio of the distance between the spring and support point to that between the mass block and support point
β	constant ratio of the distance between the active control force and mass block to that between the spring and mass block, $L_{T1j} + L_{T2j}$
β_j	ratio of the distance between the active control force and mass block to that between the spring and mass block, $L_{T1j} + L_{T2j}$
η_j	normalized mass moment of inertia of the jth lever
λ	ratio of the external excitation frequency to the structural frequency corresponding to the vibration mode being controlled, which is set within the range from 0.4 to 3.4
ξ_s	structural damping ratio, which is set in this paper equal to 0.02
ξ_T	average damping ratio of the LT-AMTMD
ξ_{Tj}	damping ratio of the jth LT-ATMD in the LT-AMTMD
μ	constant ratio of the lever mass to block mass of the LT-AMTMD
μ_j	lever mass to block mass ratio of the jth LT-ATMD in the LT-AMTMD
μ_T	total mass ratio of the LT-AMTMD
μ_{Tj}	mass ratio of the jth LT-ATMD in the LT-AMTMD
ω	external excitation frequency
ω_s	structural natural frequency corresponding to the vibration mode being controlled
ω_T	average natural frequency of the LT-AMTMD
ω_{Tj}	natural frequency of the jth LT-ATMD in the LT-AMTMD

2. Transfer functions (TFs) of the LT-AMTMD structure system

In the present paper, the LT-AMTMD is taken into account for the control of the specific vibration mode of a structure. Likewise, only the translation degree of freedom for the dynamic response of the structure
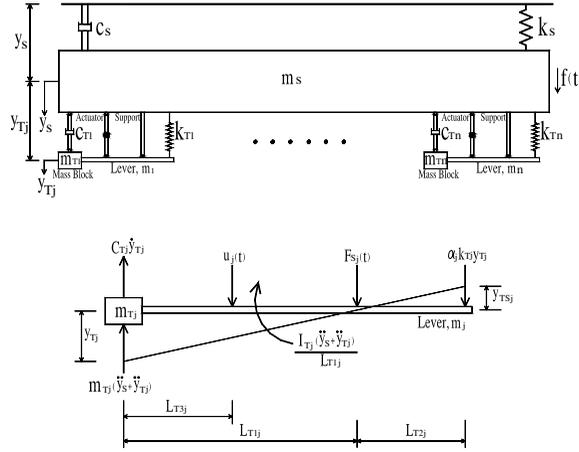
Figure 1. Schematic diagram of the lever-type active multiple tuned mass dampers (LT-AMTMD) structure system under the external excitation directly acting on the structure rather than through the base.

is taken into consideration. The structure is modeled as a single degree of freedom (SDOF) system, generally referred to as the main system, characterized by the mode-generalized dynamic parameters. Each LT-ATMD, with different dynamic characteristics, is also modeled as an SDOF system. Further, the lever is supposed to be a rigid arm. As a result, the total number of degrees of freedom of this combined system is $n+1$, as shown in Figure 1, in which n denotes the total number of the LT-ATMD units in the LT-AMTMD. Introducing the nondimensional parameters

$$\alpha_j = \frac{L_{T2j}}{L_{T1j}} \quad \text{and} \quad \beta_j = \frac{L_{T3j}}{L_{T1j} + L_{T2j}},$$

in which L_{T1j} represents the distance between the mass block and support point of the jth LT-ATMD in the LT-AMTMD, L_{T2j} denotes the distance between the spring and support point of the jth LT-ATMD in the LT-AMTMD, and L_{T3j} is the distance between the active control force and mass block of the jth LT-ATMD in the LT-AMTMD, the dynamic stretching of each spring and the location of each active control force in the LT-AMTMD can be, respectively, determined by

$$y_{TSj} = \alpha_j y_{Tj}, \tag{1a}$$

$$L_{T3j} = [(1+\alpha_j)\beta_j]L_{T1j}, \tag{1b}$$

in which y_{Tj} is the displacement of each LT-ATMD in the LT-AMTMD with reference to the structure.

Each LT-ATMD spring stroke, namely the dynamic stretching, can be calculated using Equation (1a), consequently meaning that $R_{IIj}^* = \alpha_j R_{IIj}$, in which R_{IIj}^* represents the spring stroke of the jth LT-ATMD in the LT-AMTMD and R_{IIj} denotes the mass block stroke of the jth LT-ATMD in the LT-AMTMD to

be defined next. The equations of motion of the LT-AMTMD structure system can be given by

$$I_{Tj}\big[(\ddot{y}_s + \ddot{y}_{Tj})/L_{T1j}\big] + \big[m_{Tj}(\ddot{y}_s + \ddot{y}_{Tj}) + c_{Tj}\dot{y}_{Tj}\big]L_{T1j}$$

$$+\alpha_j k_{Tj} y_{Tj} L_{T2j} = u_j(t)(L_{T1j} - L_{T3j}),$$

$$\alpha_j k_{Tj} y_{Tj} + F_{sj}(t) + u_j(t) = c_{Tj}\dot{y}_{Tj} + m_{Tj}(\ddot{y}_s + \ddot{y}_{Tj}),$$

$$m_s \ddot{y}_s + c_s \dot{y}_s + k_s y_s = f(t) + \sum_{j=1}^{n} F_{cj}(t), \tag{2}$$

$$F_{cj}(t) = c_{Tj}\dot{y}_{Tj} - u_j(t) - F_{sj}(t) - \alpha_j k_{Tj} y_{Tj} = -m_{Tj}(\ddot{y}_s + \ddot{y}_{Tj}).$$

An active control algorithm is required to use the measured displacement, velocity, and acceleration responses of the LT-AMTMD structure system to calculate the active control forces to drive the levers or the mass blocks during the design process of the LT-AMTMD. In the present paper, the frequency domain design method [Chang and Yang 1995; Ankireddi and Yang 1996; Yan et al. 1999] is employed for designing the LT-AMTMD. In this method, the optimum LT-MTMD, as obtained earlier, is utilized. For designing the LT-AMTMD, choices are displacement feedback, velocity feedback, and acceleration feedback. Such a LT-AMTMD control system, if properly designed, can be used to bring the system performance to another optimum state. Therefore, the active force $u_j(t)$ is calculated from the displacement, velocity, and acceleration of the mass block of the jth LT-ATMD in the following form:

$$u_j(t) = -m_{tj}\ddot{y}_{Tj} - c_{tj}\dot{y}_{Tj} - k_{tj} y_{Tj}, \tag{3}$$

where m_s, c_s, and k_s are, respectively, the mode-generalized stiffness, damping coefficient, and mass of structures; m_{Tj}, c_{Tj}, and k_{Tj} are the mass, damping coefficient, and stiffness of the jth LT-ATMD in the LT-AMTMD, respectively; y_s is the structural displacement relative to the ground; $F_{sj}(t)$ is the interaction force between the structure and the support point of each LT-ATMD in the LT-AMTMD;

$$I_{Tj} = \frac{[3(1 - \alpha_j)^2 + (1 + \alpha_j)^2]m_j L_{T1j}^2}{12}$$

is the mass moment of inertia of each lever in the LT-AMTMD, where m_j is the mass of each lever; $f(t)$ is the external excitation; m_{tj} is the acceleration feedback gain of the jth LT-ATMD in the LT-AMTMD; c_{tj} is the velocity feedback gain of the jth LT-ATMD in the LT-AMTMD; and k_{tj} is the displacement feedback gain of the jth LT-ATMD in the LT-AMTMD.

It is pointed out herein that this is the external excitation directly acting on the structure, rather than through the base. The main purpose of selecting this form of excitation is to give guidelines for the buffeting control design of long-span bridges under wind loads.

It is assumed that the stiffness and damping coefficient of each LT-ATMD in the LT-AMTMD are kept same and the natural frequencies of the LT-AMTMD are uniformly distributed around their average natural frequency. As a result, the LT-AMTMD is manufactured by keeping constant stiffness and damping and unequal masses (that is, $k_{T1} = k_{T2} = \cdots = k_{Tn} = k_T$; $c_{T1} = c_{T2} = \cdots = c_{Tn} = c_T$;

$m_{T1} \neq m_{T2} \neq \cdots \neq m_{Tn}$). Likewise, the nondimensional parameter α_j and β_j are, respectively, assumed to be maintained constant (that is, $\alpha_1 = \alpha_2 = \cdots = \alpha_n = \alpha$; $\beta_1 = \beta_2 = \cdots = \beta_n = \beta$).

In the formulation of the transfer functions (TFs), the following parameters are introduced:

$$\eta_j = \frac{3(1 - \alpha_j)^2 + (1 + \alpha_j)^2}{12},$$

(in physical terms $\eta_1 = \eta_2 = \cdots = \eta_n = \eta$);

$$\omega_s = \sqrt{\frac{k_s}{m_s}}, \qquad \xi_s = \frac{c_s}{2m_s\omega_s}, \qquad \omega_{Tj} = \sqrt{\frac{\alpha_j^2 k_{Tj} + k_{tj}(1 - \beta_j - \alpha_j\beta_j)}{m_{Tj}}},$$

$$\xi_{Tj} = \frac{c_{Tj} + c_{tj}(1 - \beta_j - \alpha_j\beta_j)}{2m_{Tj}\omega_{Tj}}, \qquad r_j = \frac{m_{tj}}{m_{Tj}}, \tag{4}$$

(normalized acceleration feedback gain factor, referred to as NAFGF, letting $r_1 = r_2 = \cdots = r_n = r$); $\mu_{Tj} = \frac{m_{Tj}}{m_s}$ (mass ratio of each LT-ATMD in the LT-AMTMD); $\mu_j = \frac{m_j}{m_{Tj}}$ (lever mass to block mass ratio of each LT-ATMD in the LT-AMTMD). Let it be supposed that the lever mass to block mass ratio of each LT-ATMD in the LT-AMTMD is held constant (that is, $\mu_1 = \mu_2 = \cdots = \mu_n = \mu$).

Letting $f(t) = m_s[e^{-i\omega t}]$, $y_{Tj} = [H_{y_{Tj}}(-i\omega)][e^{-i\omega t}]$ and $y_s = [H_{y_s}(-i\omega)][e^{-i\omega t}]$, and setting these in Equation (2), the transfer functions (TFs) of the LT-AMTMD structure system can then be given by

$$\omega_s^2[H_{y_s}(-i\omega)] = \frac{1}{[\mathrm{Re}(\omega) + i\,\mathrm{Im}(\omega)]}, \tag{5}$$

$$\omega_s^2[H_{y_{Tj}}(-i\omega)] = \frac{(1 + \eta_j\mu_j)[\omega^2/\omega_s^2]}{[\overline{\mathrm{Re}}(\omega) + i\overline{\mathrm{Im}}(\omega)][\mathrm{Re}(\omega) + i\,\mathrm{Im}(\omega)]}, \tag{6}$$

in which $H_{y_s}(-i\omega)$ refers to the transfer function (TF) of the structure with the LT-AMTMD; $H_{y_{Tj}}(-i\omega)$ signifies the transfer function (TF) of the jth LT-ATMD in the LT-AMTMD; and $\mathrm{Re}(\omega)$, $\mathrm{Im}(\omega)$, $\overline{\mathrm{Re}}(\omega)$, and $\overline{\mathrm{Im}}(\omega)$ will be given next.

Lastly, it is pointed out that [Li and Wang 2003] have performed numerical simulations of the lever-type multiple tuned dampers (LT-MTMD) in the case of ignoring the lever mass effect. Recently, [Li and Li 2005] have again evaluated the optimal performance of the LT-MTMD under the circumstances of taking the lever moment effect into consideration and ignoring both the inertial force and corresponding moment due to the lever mass. The numerical simulations demonstrate that the lever mass may be set equal to zero in designing the LT-AMTMD. For the LT-AMTMD, the ratio of the inertial force due to lever mass to that of block mass may be given by

$$R_{m1} = \frac{\mu_j[\ddot{y}_s + 0.5(1 - \alpha_j)\ddot{y}_{Tj}]}{(\ddot{y}_s + \ddot{y}_{Tj})},$$

whereas the ratio of the moment of inertial force due to lever mass to that of block mass around the horizontal axis through the support point of the lever can be determined by

$$R_{m2} = \frac{\mu_j[0.5(1-\alpha_j)\ddot{y}_s + 0.25(1-\alpha_j)^2\ddot{y}_{Tj}]}{(\ddot{y}_s + \ddot{y}_{Tj})}.$$

Therefore, both the inertial force and corresponding moment due to lever mass are also ignored in the present paper according to recommendations of the foregoing literatures [Li and Li 2005; Li and Wang 2003] and considering aforementioned two ratios.

3. Optimum criteria of the LT-AMTMD

Let ω_T be the average frequency of the LT-AMTMD, that is,

$$\omega_T = \sum_{k=1}^{n} \frac{\omega_{Tk}}{n}.$$

The natural frequency of each LT-ATMD in the LT-AMTMD can be derived as follows:

$$\omega_{Tj} = \omega_T\left[1 + \left[j - \frac{n+1}{2}\right]\frac{F_S}{n-1}\right], \tag{7}$$

in which the nondimensional parameter F_S is defined to be the frequency spacing of the LT-AMTMD (used for estimating the robustness of the LT-AMTMD) determined by

$$F_S = \left[\frac{\omega_{Tn} - \omega_{T1}}{\omega_T}\right].$$

Then, the ratio of the natural frequency of each LT-ATMD in the LT-AMTMD to the controlled frequency of the structure can be written as follows:

$$r_{Tj} = \frac{\omega_{Tj}}{\omega_s} = f\left[1 + \left[j - \frac{n+1}{2}\right]\frac{F_S}{n-1}\right], \tag{8}$$

in which f is defined to be the tuning frequency ratio of the LT-AMTMD calculated by $f = \frac{\omega_T}{\omega_s}$.

The average damping ratio of the LT-AMTMD is defined as follows:

$$\xi_T = \sum_{j=1}^{n} \frac{\xi_{Tj}}{n}. \tag{9}$$

The ratio of the total mass of the LT-AMTMD to the mode-generalized mass of the structure is referred to as the total mass ratio of the LT-AMTMD, which has the form

$$\mu_T = \sum_{j=1}^{n} \frac{m_{Tj}}{m_s} = \sum_{j=1}^{n} \mu_{Tj}. \tag{10}$$

Employing the above assumptions and derived expressions, the total mass ratio of the LT-AMTMD and the damping ratio of each LT-ATMD in the LT-AMTMD can be, respectively, determined as [Li

2000]

$$\mu_T = \left[\mu_{Tj} r_{Tj}^2\right]\left[\sum_{j=1}^{n} r_{Tj}^{-2}\right], \tag{11}$$

$$\xi_{Tj} = \frac{r_{Tj}\xi_T}{f}. \tag{12}$$

Defining the ratio of the external excitation frequency to the controlled frequency of the structure (that is, $\lambda = \omega/\omega_s$) and taking advantage of Equation (5) and (6), the dynamic magnification factors (DMF) of the structure with the LT-AMTMD and each LT-ATMD in the LT-AMTMD can then be respectively calculated by

$$\text{DMF} = |\omega_s^2[H_{y_s}(-i\lambda)]| = \frac{1}{\sqrt{[\text{Re}(\lambda)]^2 + [\text{Im}(\lambda)]^2}},$$

$$\text{DMF}_j = |\omega_s^2[H_{y_{Tj}}(-i\lambda)]| = \frac{(1 + \eta_j\mu_j)\lambda^2}{\sqrt{[\overline{\text{Re}}(\lambda)]^2 + [\overline{\text{Im}}(\lambda)]^2}\sqrt{[\text{Re}(\lambda)]^2 + [\text{Im}(\lambda)]^2}},$$

in which

$$\text{Re}(\lambda) = 1 - (1 + \mu_T)\lambda^2 - \sum_{j=1}^{n} \frac{[\mu_{Tj}(1 + \eta_j\mu_j)\lambda^4]\overline{\text{Re}}(\lambda)}{[\overline{\text{Re}}(\lambda)]^2 + [\overline{\text{Im}}(\lambda)]^2},$$

$$\text{Im}(\lambda) = -2\xi_s\lambda + \sum_{j=1}^{n} \frac{[\mu_{Tj}(1 + \eta_j\mu_j)\lambda^4]\overline{\text{Im}}(\lambda)}{[\overline{\text{Re}}(\lambda)]^2 + [\overline{\text{Im}}(\lambda)]^2},$$

$$\overline{\text{Re}}(\lambda) = r_{Tj}^2 - \left[1 + \eta_j\mu_j + r_j(1 - \beta_j - \alpha_j\beta_j)\right]\lambda^2,$$

$$\overline{\text{Im}}(\lambda) = -2\xi_{Tj}r_{Tj}\lambda.$$

Estimation can now be conducted on the optimum parameters and effectiveness of the LT-AMTMD through the implementation of the following optimum criterion:

$$R_I = \min.\min.\max.\text{DMF}(F_s, f, \xi_T). \tag{13}$$

Equation (13) means that the examination of the optimum parameters is conducted through the minimization of the minimum values of the maximum dynamic magnification factors (DMF) of structures with the LT-AMTMD. They can be explicitly explained in the following steps. First of all, for a fixed value of λ (set in the present paper within the range from 0.4 to 3.4) and a fixed tuning frequency ratio, the maximum amplitudes for different average damping ratios and frequency spacings are found, and the minimum amplitudes are selected from the maximum amplitudes, which is the minimax amplitude for that tuning frequency ratio. Then the above procedure is repeated for different tuning frequency ratios to find the minimax of each tuning frequency ratio. Finally, the smallest minimaxes are selected and the corresponding tuning frequency ratio, average damping ratio, and frequency spacing are optimum values.

Control systems	Units comprising the control systems				
LT-AMTMD	LT-ATMD1	LT-ATMD2	LT-ATMD3	LT-ATMD4	LT-ATMD5
Hanging-type AMTMD	Hanging-type ATMD1	Hanging-type ATMD2	Hanging-type ATMD3	Hanging-type ATMD4	Hanging-type ATMD5
LT-MTMD	LT-TMD1	LT-TMD2	LT-TMD3	LT-TMD4	LT-TMD5
Hanging-type MTMD	Hanging-type TMD1	Hanging-type TMD2	Hanging-type TMD3	Hanging-type TMD4	Hanging-type TMD5

Table 1. The control systems and units comprising these control systems

Estimation on the mass block stroke the LT-AMTMD can be simultaneously performed in terms of the maximum dynamic magnification factor ($\mathrm{Max.DMF}_j$) of each LT-ATMD using the obtained optimum parameters of the LT-AMTMD based on Equation (13), which has the following form:

$$R_{II\,j} = \mathrm{Max.DMF}_j. \tag{14}$$

It is further pointed out here that in this study, a frequency domain analysis is conducted to demonstrate the performance of the LT-AMTMD, thus implying that the aforesaid R_I and $R_{II\,j}$ can be considered as the formal indices.

4. Numerical simulation study

Displayed in Figures 2–8 are the numerical results of the present research, in which the structural damping ratio is set equal to 0.02 and the ratio (λ) of the external excitation frequency to the structural controlled frequency is set within the range from 0.4 to 3.4. The superscript *opt* represents the optimum values of the LT-AMTMD system parameters. By optimizing R_I, the optimum frequency spacing, tuning frequency ratio, and average damping ratio of the LT-AMTMD will be obtained. It is worth mentioning that the numerical analysis may be carried out of the LT-AMTMD with 5 LT-ATMD units, due to economical reasons that the number of LT-ATMD units should be as low as possible. However, to disclose the performance of the LT-AMTMD more clearly, the present paper will display the charts of the LT-AMTMD with up to 31 LT-ATMD units. For the sake of clarity, Table 1 presents the control systems and units comprising these control systems.

4.1. *Estimating the optimum locations of the actuator in the LT-AMTMD.* It is interesting in observing Figure 2 [(a1) and (b1)] to note that changing the locations of the actuator makes little difference in the optimum average damping ratio of the LT-AMTMD. It is seen that the optimum average damping ratio of the LT-AMTMD is greater than that of the LT-MTMD, but is significantly lower than the optimum damping ratio of a single LT-ATMD. From Figure 2 [(a2) and (b2)], it is important to note that the LT-AMTMD with the actuator set at the mass block offers higher robustness in comparison to the LT-AMTMD with the actuator set at any other locations. Likewise, this LT-AMTMD with the actuator set at
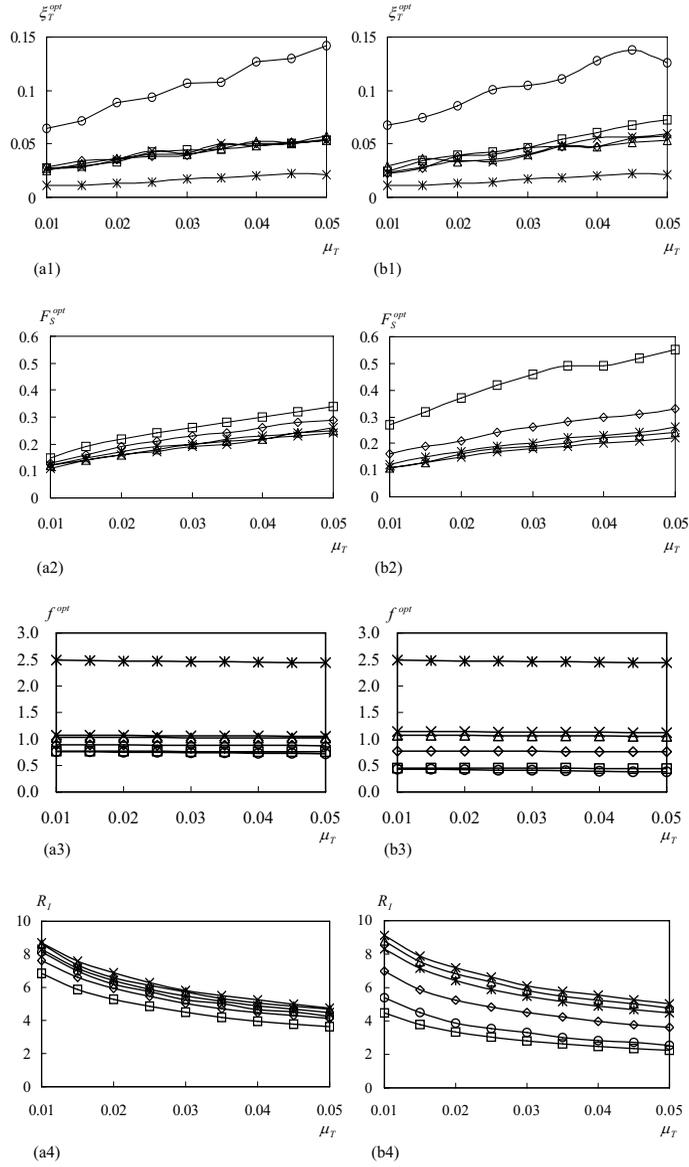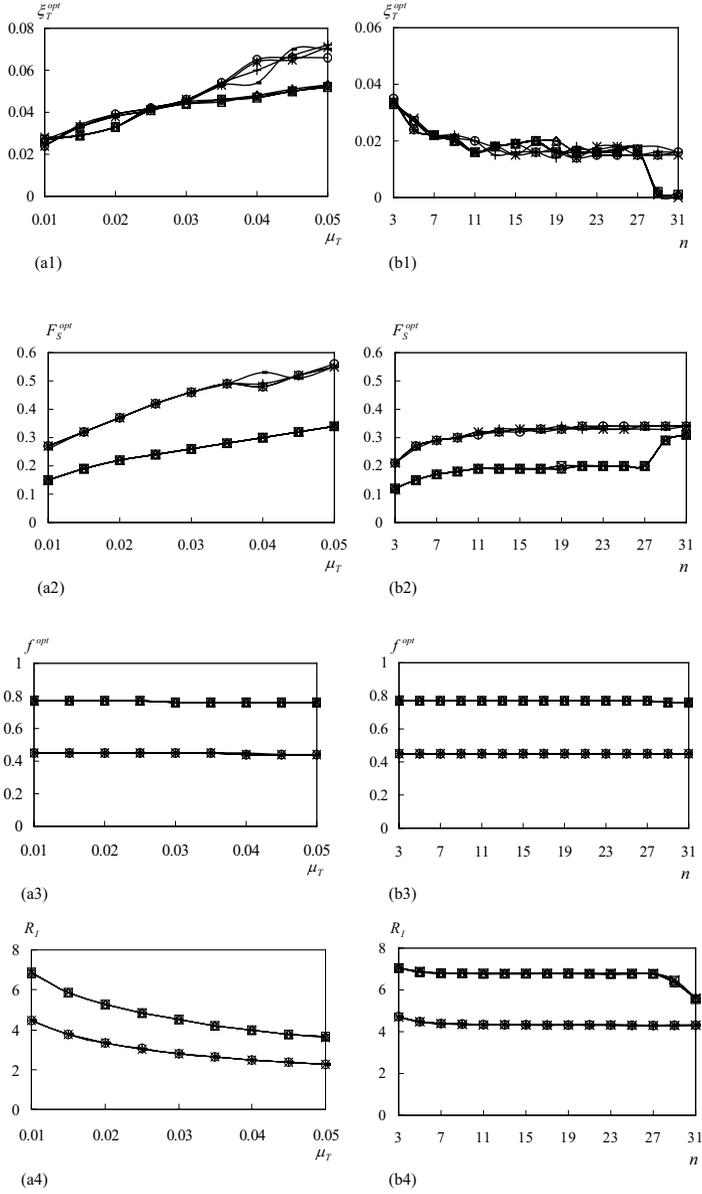
Figure 2. Variation of the optimum parameters and effectiveness of the LT-AMTMD / LT-MTMD (the passive counterpart of the LT-AMTMD) / a single LT-ATMD. (a1) ξ_T^{opt} for $r = -0.4$; (b1) ξ_T^{opt} for $r = -0.8$; (a2) F_S^{opt} for $r = -0.4$; (b2) F_S^{opt} for $r = -0.8$; (a3) f^{opt} for $r = -0.4$; (b3) f^{opt} for $r = -0.8$; (a4) R_I for $r = -0.4$; (b4) R_I for $r = -0.8$ with respect to total mass ratio with $n = 5$, $\alpha = 0.4$, $\mu = 0.01$, and several β values (considering the changes of actuator locations). Legend: $\square$ = LT-AMTMD ($\beta = 0.0$); $\diamondsuit$ = LT-AMTMD ($\beta = 0.36$); $\triangle$ = LT-AMTMD ($\beta = 0.86$); $\times$ = LT-AMTMD ($\beta = 1.0$); $\star$ = LT-MTMD; $\bigcirc$ = LT-ATMD ($\beta = 0$).

the mass block renders higher robustness in comparison with the LT-MTMD. It is seen from Figure 2 [(a3) and (b3)] that the influence of the locations of the actuator is not insignificant on the optimum tuning frequency ratio of the LT-AMTMD. Further, the optimum tuning frequency ratio of the LT-AMTMD is considerably close to that of a single LT-ATMD when both actuators are all set at the mass block, but is remarkably lower than that of the LT-MTMD. Figure 2 [(a4) and (b4)] clearly demonstrates that the LT-AMTMD with the actuator set at the mass block results in higher effectiveness compared to the LT-AMTMD with the actuator set at any other locations. The LT-AMTMD with the actuator set at the mass block can provide better effectiveness in comparison with the LT-MTMD and a single LT-ATMD. Therefore, it is preferable to choose to use the LT-AMTMD with the actuator set at the mass block.
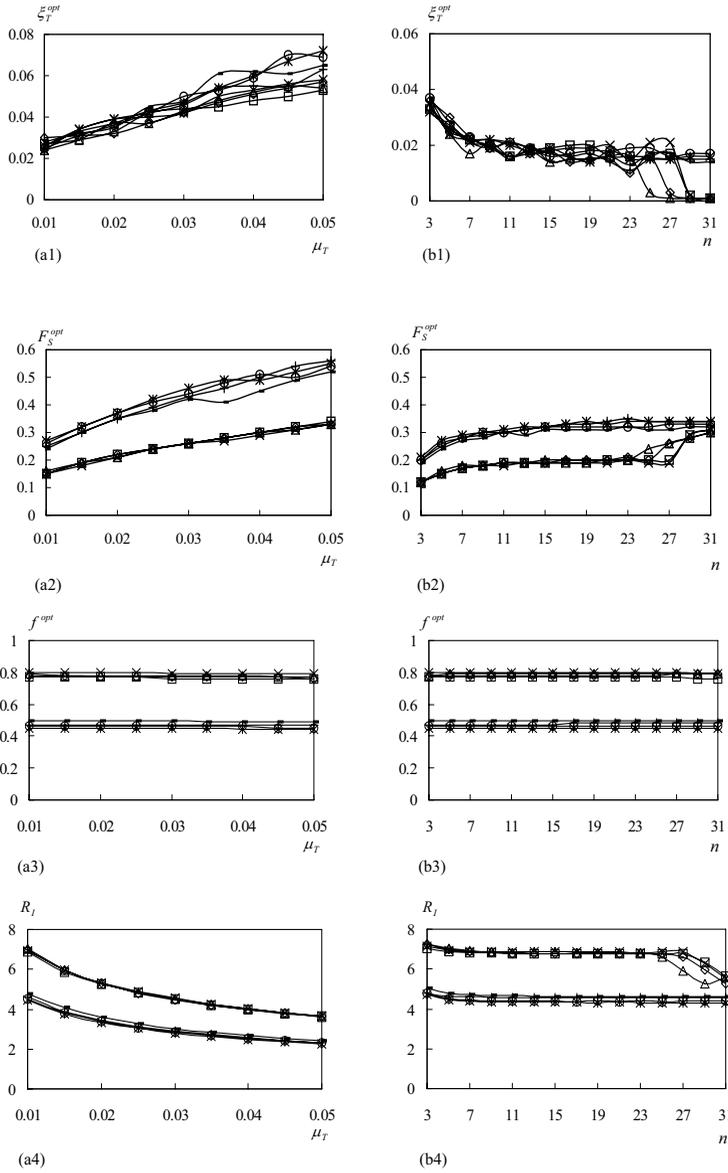
4.2. *Estimating the optimum parameters and effectiveness of the LT-AMTMD with the actuator set at the mass block.* It is interesting in observing Figure 3 to find that the locations of the support makes little difference in the optimum parameters and effectiveness of the LT-AMTMD, corresponding to the respective NAFGF. This observation effectively means that both the static and dynamic stretching of the spring in the LT-AMTMD may be freely adjusted in accordance with the practical requirements through changing the locations of the support while practically maintaining the same optimum average damping ratio, frequency spacing, tuning frequency ratio, and effectiveness. It is clear from Figure 4 that the lever mass to block mass ratio makes little difference in the optimum parameters and effectiveness of the LT-AMTMD. This effectively means the influences of the lever mass are rather negligible on the optimum parameter and effectiveness of the LT-AMTMD.

4.3. *Estimating the mass block stroke of the LT-AMTMD with the actuator set at the mass block.* Figure 5 [(a1) and (b1)] clearly illustrates that the influence of the α value within the range from 0.3 to 0.7 is rather negligible on the R_{IIj} value of the LT-AMTMD, but not insignificant out of the range. Thus, both the static and dynamic stretching of the spring in the LT-AMTMD may be freely adjusted in accordance with the practical requirements through changing the location of the support within the range from $\alpha = 0.3$ to $\alpha = 0.7$ while practically maintaining the same mass block stroke. This character is very useful for the implementation of the LT-AMTMD for long-span bridges. It is seen from Figure 5 [(a2) and (b2)] that the influence of the μ value is rather negligible on the R_{IIj} value of the LT-AMTMD at smaller NAFGF such as $r = -0.8$, but not insignificant at higher NAFGF such as $r = -0.4$. In order to more accurately estimate the mass block stroke, the lever mass thus needs to be accounted for. It is seen from Figure 5 [(a3) and (b3)] that the R_{IIj} value of the LT-AMTMD decreases rapidly with the increase of the total mass ratio, which implies that the mass block stroke of the LT-AMTMD is greatly reduced at higher total mass ratio. However, the gradient of mass block stroke reduction becomes small in the case where the total mass ratio is beyond 0.03. It is important to emphasize that the NAFGF makes little difference in the mass block stroke of the LT-AMTMD.

4.4. *Estimating the frequency response functions (FRFs) of the structures with the LT-AMTMD with the actuator set at the mass block.* It is seen from Figure 6 that the FRFs of the structures with the LT-AMTMD for different α values are very consistent with each other, thus meaning that changing the support locations practically has no influence on the FRFs of the structures with the LT-AMTMD. Likewise the FRFs of the structures with the LT-AMTMD are very consistent with those of the hanging-type AMTMD. Figure 7 is presented to take into account the effects of the mass ratio (μ) on the FRFs

Figure 3. Variation of the optimum parameters and effectiveness of the LT-AMTMD with the actuator set at the mass block with respect to total mass ratio with $n = 5$ and $\mu = 0.01$. (a1) ξ_T^{opt}; (a2) F_S^{opt}; (a3) f^{opt}; (a4) R_I and total number with $\mu_T = 0.01$ and $\mu = 0.01$ (b1) ξ_T^{opt}; (b2) F_S^{opt}; (b3) f^{opt}; (b4) R_I. Legend: $\square$ = LT-AMTMD ($\alpha = 0.1$, $\gamma = -0.4$); $\diamond$ = LT-AMTMD ($\alpha = 0.3$, $\gamma = -0.4$); $\triangle$ = LT-AMTMD ($\alpha = 0.5$, $\gamma = -0.4$); $\times$ = LT-AMTMD ($\alpha = 1.0$, $\gamma = -0.4$); $\star$ = LT-AMTMD ($\alpha = 0.1$, $\gamma = -0.8$); $\bigcirc$ = LT-AMTMD ($\alpha = 0.3$, $\gamma = -0.8$); ı = LT-AMTMD ($\alpha = 0.5$, $\gamma = -0.8$); $-$ = LT-AMTMD ($\alpha = 1.0$, $\gamma = -0.8$).

Figure 4. Variation of the optimum parameters and effectiveness of the LT-AMTMD with the actuator set at the mass block with respect to total mass ratio with $n = 5$ and $\alpha = 0.4$ (a1) ξ_T^{opt}; (a2) F_S^{opt}; (a3) f^{opt}; (a4) R_I and total number with $\mu_T = 0.01$ and $\alpha = 0.4$ (b1) ξ_T^{opt}; (b2) F_S^{opt}; (b3) f^{opt}; (b4) R_I. Legend: $\square$ = LT-AMTMD ($\mu = 0.01$, $\gamma = -0.4$); $\diamond$ = LT-AMTMD ($\mu = 0.05$, $\gamma = -0.4$); $\triangle$ = LT-AMTMD ($\mu = 0.1$, $\gamma = -0.4$); $\times$ = LT-AMTMD ($\mu = 0.2$, $\gamma = -0.4$); $\star$ = LT-AMTMD ($\mu = 0.01$, $\gamma = -0.8$); $\circ$ = LT-AMTMD ($\mu = 0.05$, $\gamma = -0.8$); $\shortmid$ = LT-AMTMD ($\mu = 0.1$, $\gamma = -0.8$); $-$ = LT-AMTMD ($\mu = 0.2$, $\gamma = -0.8$).
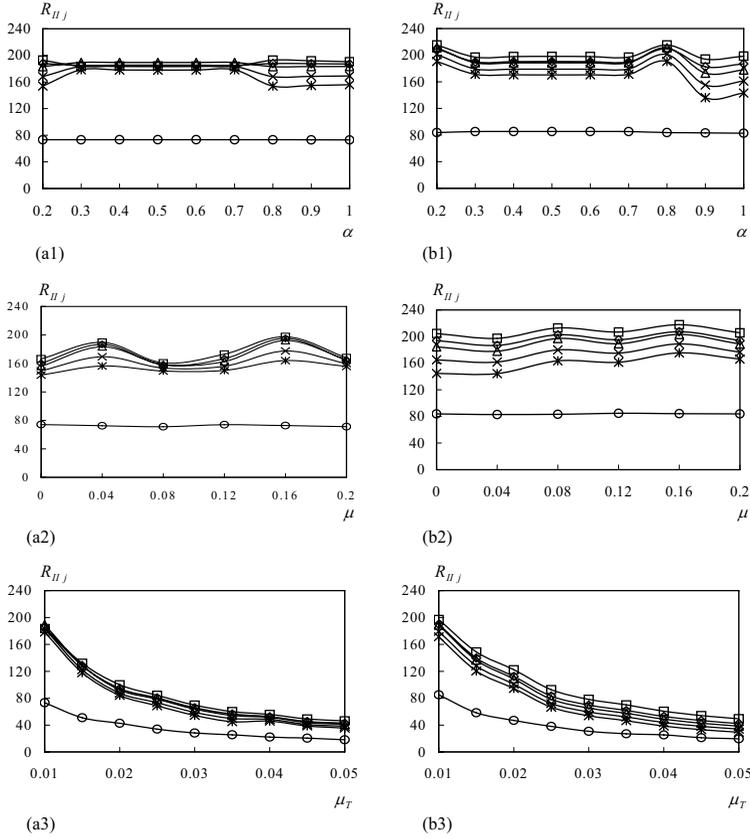
Figure 5. Variation of the R_{IIj} value of the LT-AMTMD / a single LT-ATMD with the actuator set at the mass block with respect to the α value with $n = 5$ and $\mu_T = 0.01$ and $\mu = 0.03$. (a1) $r = -0.4$; (b1) $r = -0.8$ and the μ value with $n = 5$ and $\mu_T = 0.01$ and $\alpha = 0.3$; (a2) $r = -0.4$; (b2) $r = -0.8$ and the μ_T value with $n = 5$ and $\alpha = 0.3$ and $\mu = 0.03$; (a3) $r = -0.4$; (b3) $r = -0.8$. Legend: $\square$ = LT-ATMD1; $\diamond$ = LT-ATMD2; $\triangle$ = LT-ATMD3 $\times$ = LT-ATMD4; $\star$ = LT-ATMD5; $\circ$ = LT-ATMD.

of the structures with the LT-AMTMD. For smaller NAFGF, the FRFs of the structures with the LT-AMTMD are almost identical to each other for different μ values even though greater total mass ratio, such as $\mu_T = 0.03$. For greater NAFGF, the mass ratio (μ) has an effect on the FRFs of the structures with the LT-AMTMD, but not significant as well. Figure 8 exhibits the effects of the actuator locations (β) on the FRFs of the structures with the LT-AMTMD. It is seen that the actuator locations significantly affects the FRFs of the structures with the LT-AMTMD. With the increase in the β value, the FRFs of the structures with the LT-AMTMD are getting worse. Therefore, the LT-AMTMD with the actuator set at the mass block will yield the best performance.
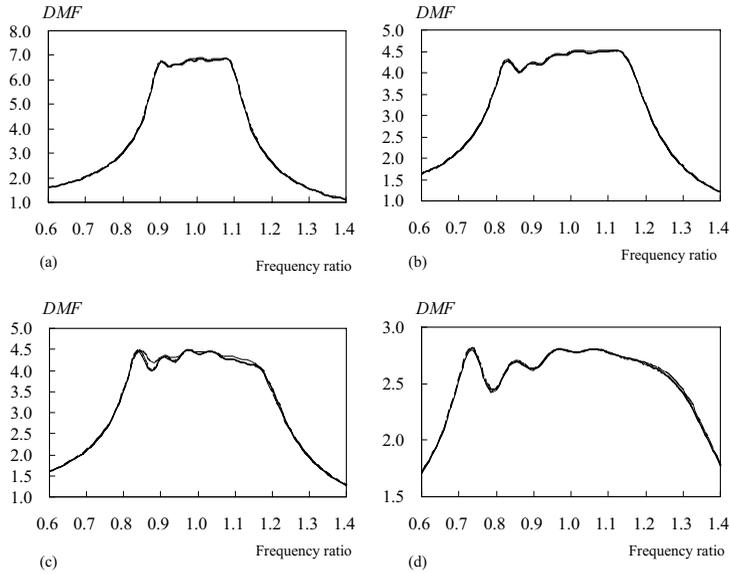
Figure 6. FRFs of the structures with the LT-AMTMD with the actuator set at the mass block with $n = 5$, $\mu = 0.01$, and several α values (considering the changes of the support locations) and with (a) $r = -0.4$ and $\mu_T = 0.01$; (b) $r = -0.4$ and $\mu_T = 0.03$; (c) $r = -0.8$ and $\mu_T = 0.01$; and (d) $r = -0.8$ and $\mu_T = 0.03$. Legend:— $\alpha = 0.1$; $--\alpha = 0.3$; - - - $\alpha = 0.5$;—-- —$\alpha = 1.0$
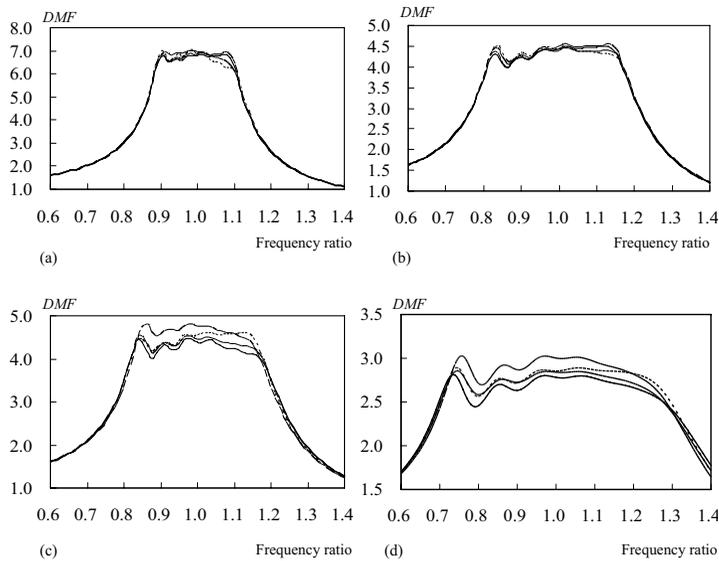
Figure 7. FRFs of the structures with the LT-AMTMD with the actuator set at the mass block with $n = 5$, $\alpha = 0.4$, and several μ values (considering the changes of lever mass) and with (a) $r = -0.4$ and $\mu_T = 0.01$; (b) $r = -0.4$ and $\mu_T = 0.03$; (c) $r = -0.8$ and $\mu_T = 0.01$; and (d) $r = -0.8$ and $\mu_T = 0.03$. Legend:— $\mu = 0.01$; $--\mu = 0.05$; - - - $\mu = 0.10$;—-- —$\mu = 0.20$.
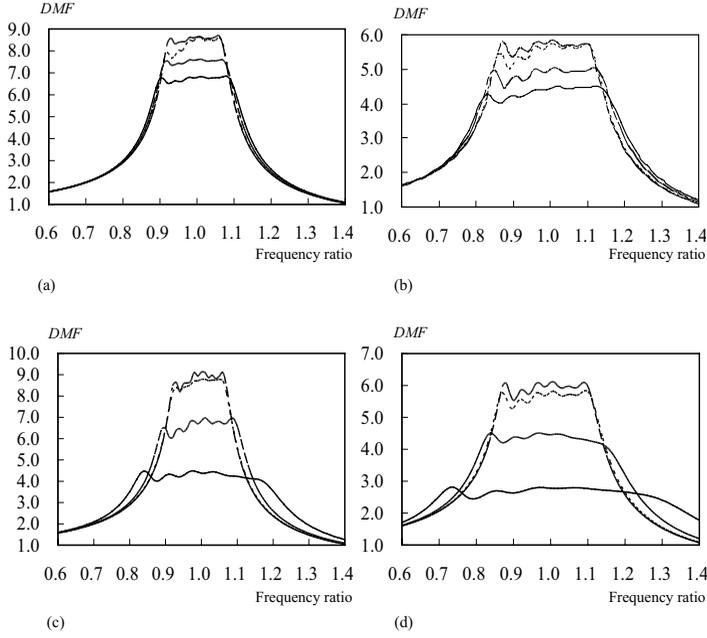
Figure 8. FRFs of the structures with the LT-AMTMD with $n = 5$, $\alpha = 0.4$, $\mu = 0.01$, and several β values (considering the changes of actuator locations) and with (a) $r = -0.4$ and $\mu_T = 0.01$; (b) $r = -0.4$ and $\mu_T = 0.03$; (c) $r = -0.8$ and $\mu_T = 0.01$; and (d) $r = -0.8$ and $\mu_T = 0.03$. Legend: — $\beta = 0.0$; — — $\beta = 0.36$; - - - $\beta = 0.86$; —·· — $\beta = 1.0$.

4.5. *Estimating the performance of the LT-AMTMD / a single LT-ATMD with respect to the hanging-type AMTMD / a single hanging-type ATMD.* From Tables 2 and 3, the LT-AMTMD / a single LT-ATMD has approximately the same performances as the hanging-type AMTMD / a single hanging-type ATMD. The mass block stroke of the LT-AMTMD is slightly greater than that of the LT-MTMD, but is significantly larger than that of a single ATMD. Thus, in comparison to a single LT-ATMD, this is a disadvantage of the LT-AMTMD.

4.6. *Estimating the performance of the LT-MTMD (passive counterpart of the LT-AMTMD) / a single LT-TMD designed in terms of two hypotheses with respect to the hanging-type MTMD / a single hanging-type TMD.* Here, it is pointed out that in this research the natural frequency of each LT-TMD in the LT-MTMD (that is, passive counterpart of the LT-AMTMD) takes the forms:

$$\omega_{Tj} = \sqrt{k_{Tj}/m_{Tj}}$$

(designated in this paper as the hypothesis-1). If

$$\omega_{Tj} = \sqrt{\alpha_j^2 k_{Tj}/m_{Tj}}$$

(similarly designated as the hypothesis-2), which can be derived from the natural frequency expression of the LT-AMTMD by setting both $1 - \beta_j - \alpha_j\beta_j = 0$ and $r_j = 0$, then the optimum tuning frequency

NAFGF (r)	LT-ATMD1	LT-ATMD2	LT-ATMD3	LT-ATMD4	LT-ATMD5
Computational results with the total mass ratio (μ_T) equal to 0.01					
-0.2	158.67	153.22	149.81	144.34	140.82
-0.4	168.76	163.08	161.27	155.64	151.56
-0.6	204.26	197.14	195.25	185.55	177.80
-0.8	221.75	209.48	203.36	185.88	168.76
Computational results with the total mass ratio (μ_T) equal to 0.03					
-0.2	65.40	61.81	59.96	57.11	54.63
-0.4	68.81	65.64	64.59	61.27	58.42
-0.6	79.49	74.48	71.54	64.72	57.79
-0.8	80.93	72.42	67.56	59.82	51.51
NAFGF (r)	Hanging-type ATMD1	Hanging-type ATMD2	Hanging-type ATMD3	Hanging-type ATMD4	Hanging-type ATMD5
Computational results with the total mass ratio (μ_T) equal to 0.01					
-0.2	159.90	145.10	142.00	135.86	129.65
-0.4	166.42	160.18	155.99	149.60	143.67
-0.6	194.25	187.14	183.07	171.01	160.08
-0.8	204.57	194.07	184.63	165.02	144.54
Computational results with the total mass ratio (μ_T) equal to 0.03					
-0.2	64.43	60.93	59.05	55.83	52.93
-0.4	70.96	67.13	65.57	62.01	58.88
-0.6	76.09	70.92	68.94	64.73	61.15
-0.8	78.56	69.31	64.52	59.22	54.56

Table 2. The R_{IIj} value, used for estimating the mass block stroke, of the LT-AMTMD with the actuator set at the mass block / hanging-type AMTMD with $n = 5$, $\alpha = 0.4$, and $\mu = 0.01$ and with different total mass ratio and NAFGF

ratio of the LT-MTMD can be approximately calculated by $f^{opt} = \alpha$ (that of the LT - MTMD computed in terms of the hypothesis -1), whereas the optimum average damping ratio of the LT-MTMD can be approximately determined by

$$\xi_T^{opt} = \frac{[\text{that of the LT - MTMD computed in terms of the hypothesis } -1]}{\alpha},$$

from the computational results listed in Table 4.

Obviously, the LT-MTMD designed in terms of the two hypotheses practically maintains the same optimum stiffness (k_T^{opt}) and optimum damping coefficient (c_T^{opt}). Likewise, the computational results

Total mass ratio	Tuning frequency ratio	Damping ratio	R_I value	R_{II} value
Computational results of a single LT-ATMD in the case of NAFGF $(r) = -0.40$				
0.010	0.76	0.064	8.1430	73.1342
0.015	0.76	0.071	6.9885	54.5700
0.020	0.75	0.089	6.1971	40.4935
0.025	0.75	0.094	5.7432	34.6001
0.030	0.74	0.107	5.2518	28.5802
Computational results of a single LT-ATMD in the case of NAFGF $(r) = -0.80$				
0.010	0.43	0.067	5.3907	82.9899
0.015	0.43	0.074	4.5075	60.2846
0.020	0.42	0.086	3.8713	45.7221
0.025	0.41	0.101	3.5444	36.6465
0.030	0.41	0.105	3.3100	32.0467
Computational results of a single hanging-type ATMD in the case of NAFGF $(r) = -0.40$				
0.010	0.76	0.061	8.0113	74.1981
0.015	0.76	0.080	7.0768	51.8164
0.020	0.75	0.089	6.1191	40.5152
0.025	0.74	0.102	5.7826	33.3100
0.030	0.74	0.104	5.2222	29.0629
Computational results of a single hanging-type ATMD in the case of NAFGF $(r) = -0.80$				
0.010	0.43	0.063	5.2078	83.8189
0.015	0.42	0.078	4.4928	58.6995
0.020	0.42	0.085	3.9432	46.4770
0.025	0.41	0.095	3.4822	37.5096
0.030	0.40	0.110	3.2442	31.1189

Table 3. The optimum parameters and R_{II} value of a single LT-ATMD with the actuator set at the mass block / a single hanging-type ATMD and the R_I value of the structures with the LT-ATMD / hanging-type ATMD with $\alpha = 0.4$ and $\mu = 0.01$ and with different total mass ratio and NAFGF

also shows that the two hypotheses will practically provide the same optimum frequency spacing (identical to the same robustness), same R_I value (identical to the same effectiveness), and same $R_{II j}$ value (identical to the same mass block stroke) (Refer to Tables 4 and 5). It is seen from Table 6 that a single LT-TMD takes on the identical behaviors with the LT-MTMD for these two hypotheses. It is interesting in observing Tables 4–6 to note that the LT-MTMD (passive counterpart of the LT-AMTMD) / a single

Total mass ratio	Tuning frequency ratio	Average damping ratio	Frequency spacing	R_I value
Computational results of the LT-MTMD in terms of the hypothesis -1				
0.010	2.49	0.011	0.12	8.3019
0.015	2.48	0.011	0.15	7.1540
0.020	2.47	0.013	0.17	6.4203
0.025	2.47	0.014	0.19	5.8833
0.030	2.46	0.017	0.20	5.4793
Computational results of the LT-MTMD in terms of the hypothesis -2				
0.010	0.99	0.029	0.12	8.4505
0.015	0.99	0.028	0.15	7.1852
0.020	0.99	0.033	0.17	6.4101
0.025	0.99	0.037	0.19	5.9350
0.030	0.99	0.039	0.21	5.5650
Computational results of the hanging-type MTMD				
0.010	0.99	0.028	0.12	8.3754
0.015	0.99	0.035	0.14	7.1324
0.020	0.99	0.034	0.17	6.4332
0.025	0.99	0.039	0.19	5.9641
0.030	0.98	0.046	0.20	5.5414

Table 4. The optimum parameters of the LT-MTMD (the passive counterpart of the LT-AMTMD) / hanging-type MTMD and the R_I value of the structures with the LT-MTMD / hanging-type MTMD with $n = 5$, $\alpha = 0.4$, and $\mu = 0.01$ and with different total mass ratio obtained in terms of the two hypotheses

LT-TMD designed in terms of the hypotheses-2 has approximately the same performances (including the same mass block stroke) as the hanging-type MTMD / a single hanging-type TMD with equal total mass ratio.

5. Conclusions

In the present paper, the location of the mass block is not movable; only the location of the support is movable. The LT-AMTMD proposed herein is aimed to attenuate the vibration of long-span bridges under the excitation directly acting on the structure, rather than through the base. The main purpose of selecting this form of excitation is to offer guidelines for the buffeting control design of long-span bridges under wind loads. Another important objective is to carry out the numerical estimations on the LT-AMTMD / a single LT-ATMD with respect to the hanging-type AMTMD / a single hanging-type ATMD as well as on the LT-MTMD (that is, passive counterpart of the LT-AMTMD) / a single LT-TMD with reference to the hanging-type MTMD / a single hanging-type TMD. It is worth pointing out that the locations of both the mass block and support in the MALTTMD proposed by [Li and Zhou 2004] are

Total mass ratio	LT-TMD1	LT-TMD2	LT-TMD3	LT-TMD4	LT-TMD5
Computational results in terms of the hypothesis -1					
0.010	154.01	150.66	148.34	141.62	135.23
0.015	129.20	125.98	126.57	120.26	115.60
0.020	99.56	95.84	96.14	91.96	88.48
0.025	86.16	82.66	81.58	76.79	73.28
0.030	67.94	64.04	62.84	59.84	57.86
Computational results in terms of the hypothesis -2					
0.010	140.87	141.62	143.71	140.86	137.63
0.015	125.99	123.84	124.82	119.04	115.12
0.020	99.46	95.82	95.19	90.15	85.94
0.025	82.98	79.55	78.28	72.89	68.50
0.030	73.88	70.42	69.08	63.78	58.75
Total mass ratio	Hanging-type TMD1	Hanging-type TMD2	Hanging-type TMD3	Hanging-type TMD4	Hanging-type TMD5
0.010	147.03	146.32	147.67	144.03	140.40
0.015	107.02	102.59	101.23	97.03	95.04
0.020	97.12	94.10	92.90	87.42	82.70
0.025	79.39	76.36	75.06	69.59	64.41
0.030	62.09	59.82	59.25	56.81	54.68

Table 5. The R_{IIj} value, used for estimating the mass block stroke, of the LT-MTMD (the passive counterpart of the LT-AMTMD) / hanging-type MTMD with $n = 5$, $\alpha = 0.4$, and $\mu = 0.01$ and with different total mass ratio obtained in terms of the two hypotheses

all movable. Likewise, the MALTTMD is aimed to suppress the vibration of long-span bridges under the ground motions, namely the excitation through the base. From the numerical results presented, the following main conclusions can be drawn:

(1) The LT-AMTMD with the actuator set at the mass block can provide better effectiveness and higher robustness in reducing the vibrations of long-span bridges with respect to the LT-AMTMD with the actuator set at any other locations. The actuator locations significantly affect the FRFs of the structures with the LT-AMTMD and the LT-AMTMD with the actuator set at the mass block will render the best FRFs. The FRFs of the structures with the LT-AMTMD with the actuator set at the mass block are very consistent with those of the hanging-type AMTMD. Likewise, changing the support locations practically has no influence on the FRFs of the structures with the LT-AMTMD with the actuator set at the mass block.

(2) A new basic result is that both the static and dynamic stretching of the spring in the LT-AMTMD with the actuator set at the mass block may be freely adjusted in accordance with the practical requirements through changing the locations of the support within the range from $\alpha = 0.3$ to $\alpha = 0.7$ while practically maintaining the same performance (including the same mass block stroke).

Total mass ratio	Tuning frequency ratio	Damping ratio	R_I value	R_{II} value
Computational results of a single LT-TMD in terms of the hypothesis -1				
0.010	2.47	0.025	9.4510	67.7894
0.015	2.46	0.032	8.3178	47.7892
0.020	2.44	0.036	7.5204	37.7196
0.025	2.43	0.040	6.8651	31.3496
0.030	2.42	0.042	6.4355	27.4125
Computational results of a single LT-TMD in terms of the hypothesis -2				
0.010	0.99	0.066	9.5663	66.5275
0.015	0.98	0.080	8.3924	47.6999
0.020	0.98	0.090	7.5680	38.0642
0.025	0.97	0.098	6.9489	31.6057
0.030	0.97	0.104	6.5137	27.6807
Computational results of a single hanging-type TMD				
0.010	0.99	0.065	9.6623	67.0634
0.015	0.98	0.080	8.3198	47.5598
0.020	0.98	0.090	7.6252	38.1530
0.025	0.97	0.098	6.8943	31.5617
0.030	0.97	0.103	6.5625	27.8820

Table 6. The optimum parameters and R_{II} value of a single LT-TMD (the passive counterpart of the LT-ATMD) / a single hanging-type TMD and the R_I value of the structures with the LT-TMD / hanging-type TMD with $\alpha = 0.4$ and $\mu = 0.01$ and with different total mass ratio obtained in terms of the two hypotheses

(3) The LT-AMTMD with the actuator set at the mass block can largely enhance the robustness and effectiveness of the LT-MTMD and can offer higher effectiveness in comparison to a single LT-ATMD. The mass block stroke of the LT-AMTMD with the actuator set at the mass block is slightly greater than that of the LT-MTMD, but is significantly larger than that of a single LT-ATMD.

(4) The LT-MTMD designed using the two hypotheses practically maintains the same optimum stiffness and optimum damping coefficient. The two hypotheses will practically lead to the same robustness, effectiveness, and mass block stroke. Likewise, a single LT-TMD possesses the identical behaviors to the LT-MTMD corresponding to these two hypotheses.

In fact, any type of single-degree-of-freedom oscillators can be employed as the tuned mass dampers. However, the major advantage of the LT-AMTMD is that the dynamic stretching of spring (spring stroke) can be freely adjusted while practically maintaining the performance of the LT-AMTMD unchanged. The present paper is concerned with wind-induced harmonic vibrations of long span bridges. The focus is on the (vertical) flexural mode of the bridge deck. Usually under wind there are problems with the dominant flexural and torsional modes of vibration of long span bridges. It may be necessary to reduce at least two

or even more modes. Therefore, there is a need for further estimating the behaviors of the LT-AMTMD for the dominant flexural and torsional modes of vibration of long span bridges.

Acknowledgements

References

[Abe and Fujino 1994] M. Abe and Y. Fujino, "Dynamic characterization of multiple tuned mass dampers and some design formulas", *Earthquake Eng. Struc.* **23**:8 (1994), 813–835.

[Ankireddi and Yang 1996] S. Ankireddi and H. T. Y. Yang, "Simple ATMD control methodology for tall buildings subject to wind loads", *J. Struct. Eng. ASCE* **122**:1 (1996), 83–91.

[Chang and Yang 1995] C. C. Chang and H. T. Y. Yang, "Control of buildings using active tuned mass dampers", *J. Eng. Mech. ASCE* **121**:3 (1995), 355–66.

[Chen and Wu 2003] G. Chen and J. Wu, "Experimental study on multiple tuned mass dampers to reduce seismic responses of a three-storey building structure", *Earthquake Eng. Struc.* **32**:5 (2003), 793–810.

[Conti et al. 1996] E. Conti, G. Grillaud, J. Jacob, and N. Cohen, "Wind effects on the Normandie cable-stayed bridge: comparison between full aeroelastic model tests and quasi-steady analytical approach", *J. Wind Eng. Ind. Aerod.* **65**:1-3 (1996), 189–201.

[Diana et al. 1992] G. Diana, F. Cheli, A. Zasso, A. Collina, and J. Brownjohn, "Suspension bridge parameter identification in full scale test", *J. Wind Eng. Ind. Aerod.* **41**:1-3 (1992), 165–176.

[Gu and Xiang 1992] M. Gu and H. F. Xiang, "Optimization of TMD for suppressing buffeting responses of long-span bridges", *J. Wind Eng. Ind. Aerod.* **42**:1-3 (1992), 1383–1392.

[Gu et al. 1994] M. Gu, H. F. Xiang, and A. R. Chen, "A pratical method of passive TMD for suppressing wind-induced vertical buffeting of long-span cable-stayed bridges and its application", *J. Wind Eng. Ind. Aerod.* **51**:2 (1994), 203–213.

[Gu et al. 1999] M. Gu, S. R. Chen, and C. C. Chang, "Buffeting control of the Yangpu bridge using multiple tuned mass dampers", pp. 893–8 in *Proceedings of the 10th international conference on wind engineering*, edited by A. Larsem et al., A. A. Balkema, Rotterdam, 1999.

[Gu et al. 2001] M. Gu, S. R. Chen, and C. C. Chang, "Parametric study on multiple tuned mass dampers for buffeting control of Yangpu bridge", *J. Wind Eng. Ind. Aerod.* **89**:11-12 (2001), 987–1000.

[Hoang and Warnitchai 2005] N. Hoang and P. Warnitchai, "Design of multiple tuned mass dampers by using a numerical optimizer", *Earthquake Eng. Struc.* **34**:2 (2005), 125–144.

[Igusa and Xu 1994] T. Igusa and K. Xu, "Vibration control of using multiple tuned mass dampers", *J. Sound Vib.* **175**:4 (1994), 491–503.

[Jangid 1995] R. S. Jangid, "Dynamic characteristics of structures with multiple tuned mass dampers", *Struct. Eng. Mech.* **3**:5 (1995), 497–509.

[Kareem and Kline 1995] A. Kareem and S. Kline, "Performance of multiple mass dampers under random loading", *J. Struct. Eng. ASCE* **121**:2 (1995), 348–361.

[Kwon and Park 2004] S.-D. Kwon and K.-S. Park, "Suppression of bridge flutter using tuned mass dampers based on robust performance design", *J. Wind Eng. Ind. Aerod.* **92**:11 (2004), 919–934.

[Lee et al. 2006] C.-L. Lee, Y.-T. Chen, L.-L. Chung, and Y.-P. Wang, "Optimal design theories and applications of tuned mass dampers", *Eng. Struct.* **28**:1 (2006), 43–53.

[Li 2000] C. Li, "Performance of multiple tuned mass dampers for attenuating undesirable oscillations of structures under the ground acceleration", *Earthquake Eng. Struc.* **29**:9 (2000), 1405–1421.

[Li 2004] C. Li, "Evaluation of the lever-type active tuned mass damper for structures", *Struct. Control Health Monit.* **11**:4 (2004), 259–271.

[Li and Li 2005] C. Li and Q. S. Li, "Evaluation of the lever-type multiple tuned mass dampers for mitigating harmonically forced vibration", *Int. J. Struct. Stab. Dyn.* **5**:4 (2005), 641–664.

[Li and Wang 2003] C. Li and Z. Wang, "Dynamic characteristics of lever-type multiple tuned mass dampers", *Acta Mech. Solida Sin.* **24**:4 (2003), 451–455. Chinese.

[Li and Zhou 2004] C. Li and D. Zhou, "Evaluation of multiple active lever-type tuned mass dampers for structures under ground acceleration", *Eng. Struct.* **26**:3 (2004), 303–317.

[Lin et al. 2000] Y.-Y. Lin, C.-M. Cheng, and C.-H. Lee, "A tuned mass damper for suppressing the coupled flexural and torsional buffeting response of long-span bridges", *Eng. Struct.* **22**:9 (2000), 1195–1204.

[Park and Reed 2001] J. Park and D. Reed, "Analysis of uniformly and linearly distributed mass dampers under harmonic and earthquake excitation", *Eng. Struct.* **23**:7 (2001), 802–814.

[Wang and Lin 2005] J.-F. Wang and C.-C. Lin, "Seismic performance of multiple tuned mass dampers for soil-irregular building interaction systems", *Int. J. Solids Struct.* **42**:20 (2005), 5536–5554.

[Xu and Igusa 1992] K. Xu and T. Igusa, "Dynamic characteristics of multiple substructures with closely spaced frequencies", *Earthquake Eng. Struc.* **21**:12 (1992), 1059–1070.

[Yamaguchi and Harnpornchai 1993] H. Yamaguchi and N. Harnpornchai, "Fundamental characteristics of multiple tuned mass dampers for suppressing harmonically forced oscillations", *Earthquake Eng. Struc.* **22**:1 (1993), 51–62.

[Yan et al. 1999] N. Yan, C. M. Wang, and T. Balendra, "Optimal damper characteristics of atmd for buildings under wind loads", *J. Struct. Eng. ASCE* **125**:12 (1999), 1376–83.

[Yau and Yang 2004] J.-D. Yau and Y.-B. Yang, "A wideband MTMD system for reducing the dynamic response of continuous truss bridges to moving train loads", *Eng. Struct.* **26**:12 (2004), 1795–1807.

CHUNXIANG LI: li-chunxiang@vip.sina.com
Department of Civil Engineering, Shanghai University, No. 149 Yanchang Rd., Shanghai 200072, China

BINGKANG HAN: *College of Civil Engineering, Tongji University, No. 1239 Si Ping Rd., Shanghai 200092, China*